Thyroid hormones act as a timer for the postnatal maturation of parvalbumin neurons in mouse neocortex

Juan Ren[1, 3], Suzy Markossian[1], Romain Guyot[1], Denise Aubert[1], Jacques Brocard[2], Jiemin Wong[3], Frédéric Flamant[1,*], Sabine Richard[1]

[1] Ecole Normale Supérieure de Lyon, INRAE, CNRS, Institut de Génomique Fonctionnelle de Lyon, 69364 Lyon, France

[2] Universite Claude Bernard Lyon 1, CNRS UAR3444, Inserm US8, ENS de Lyon, SFR Biosciences, Lyon 69007, France

[3] Shanghai Key Laboratory of Regulatory Biology, Institute of Biomedical Sciences and School of Life Sciences, East China Normal University, 200241, Shanghai, China

[*] Corresponding author. Frederic.flamant@ens-lyon.fr Tel: 00 (33) 4 26 73 13 32

Significance statement

Thyroid hormones are crucial for neurodevelopment, but the underlying mechanisms are still unclear. In the neocortex, mutations in thyroid hormone nuclear receptors affect the maturation of GABAergic inhibitory interneurons, and in particular a subset of these neurons that express parvalbumin. We found that, during a defined postnatal development stage, thyroid hormones are essential for the maturation of parvalbumin neurons. They notably promote the formation of the perineuronal net, a specialized extracellular matrix that contributes to the maturation of neocortical networks by stabilizing synapses around parvalbumin neurons. Experimental evidence strongly suggests that thyroid hormones act as a timer to define the temporal boundaries of the well-known critical period of heightened plasticity, during which neuronal networks are shaped by experience.

Abstract

Thyroid hormones (THs) are required for proper maturation of parvalbumin-expressing GABAergic interneurons (PV neurons) in the mouse neocortex. However, the timeline of this TH action remains to be elucidated. Here, we used several mouse models expressing dominant negative mutations of the TH nuclear receptor α1 (TRα1), to better define the time window during which TH promotes the postnatal maturation of PV neurons. Histological observations revealed that TH action during the first three postnatal weeks was necessary to initiate the expression of parvalbumin and the elaboration of a specialized extracellular matrix called perineuronal net. By contrast, after the third postnatal week, TH action on PV neuron maturation appeared to be somewhat dispensable. Transcriptome analysis of neocortical GABAergic neurons identified a small set of putative target genes for TRα1. These genes are at the origin of the postnatal remodeling of the repertoire of ions channels and the elaboration of perineuronal nets. These data suggest that THs act as a timer to define the temporal boundaries of the critical period of heightened plasticity, which plays a fundamental role in the development of neuronal circuits.

Keywords

Thyroid hormones / TRα1 / PV neurons / GABAergic neurons / neocortex

Introduction

41 PV neurons are GABAergic inhibitory interneurons that play a central role in the organization of
42 neuronal circuits in the neocortex (1). They are fast-spiking and synchronize network oscillations,
43 which are thought to play an important role in information processing and memory formation. In
44 mice, PV neurons begin to express parvalbumin during the first postnatal weeks (2, 3). During this
45 time, the electrical activity of these neurons progressively increases (4) and synaptogenesis is very
46 active. This opens the so-called critical period of heightened synaptic plasticity (5) during which
47 sensory input and experience shape the neuronal networks of the neocortex. The critical period ends
48 when excessive circuit rewiring becomes actively dampened (6). Notably, the elaboration of the
49 perineuronal net (PNN) around PV neurons, a densely packed extracellular matrix enriched in
50 proteoglycans stabilizes synapses and restrict plasticity (7). Defects in PV neuron maturation during
51 the critical period cause a persistent imbalance between neuronal excitation and inhibition, which is
52 suspected to be at the origin of several pathological conditions, including attention deficit
53 hyperactivity disorder, autism, and epilepsy (8).

54 THs (including T3 or 3,3',5-triiodo-L-thyronine, and the less active precursor T4 or thyroxine) exert a
55 broad influence on brain development. They directly act on gene transcription by binding to the TRα1
56 and TRβ1/2 nuclear receptors, which are encoded by the *Thra* and *Thrb* genes in mice. Unlike
57 TRβ1/2, TRα1 is ubiquitous from early stages of development. In both humans and mice, TRα1
58 mutations have dramatic and irreversible consequences on neurodevelopment, and these
59 consequences are similar to those of TH deficiency (9-11). Although all types of neural cells are
60 directly or indirectly dependent on THs for proper terminal differentiation, previous studies have
61 revealed that in different brain regions, the cell-autonomous influence of THs is limited to a fraction
62 of neural cells, and eventually amplified by TH-dependent release of neurotrophic factors (12).

63 In the postnatal mouse neocortex, PV neurons display a high sensitivity to TRα1 mutation (13) and TH
64 deficiency (14, 15). We have previously found that expressing TRα1^{L400R}, a dominant-negative TRα1
65 receptor, only in the GABAergic lineage from an early neurodevelopmental stage, is sufficient to
66 dramatically inhibit the expression of parvalbumin and the elaboration of PNNs (16). By contrast,
67 other subtypes of neocortical GABAergic interneurons, expressing somatostatin or calretinin, are
68 much less affected. We have also recently observed that the postnatal expression of TRα1^{L400R} in PV
69 neurons has no visible effects on their maturation and has only moderate consequences on their
70 function (Ren et al., 2024). This suggests that TH signaling stimulates the maturation of PV neurons
71 during a specific time window and then becomes less important to maintain their function.
72 Accordingly, the appearance of hypothyroidism in the adult stage (14, 17) does not prevent the
73 expression of parvalbumin. Therefore, it seems that THs exert a selective action on PV neuron

74 maturation during a specific time window. However, the boundaries of this time window remain
75 elusive. Moreover, whether blocking TH signaling during development only delays or permanently
76 inhibits PV neuron maturation remains an open question.

77 To gain more insight into the timeline of TH action on PV neuron maturation, we generated novel
78 mouse models to restrict the expression of dominant-negative TRα1 receptors in GABAergic neurons
79 during specific time windows. Histological observations of parvalbumin and PNNs in the
80 somatosensory cortex allowed us to pin point a key time window for TH action around the second
81 postnatal week. A genome-wide analysis of GABAergic neuron transcriptome in the whole neocortex
82 also allowed us to identify a set of genes whose regulation is expected to be involved in TH-mediated
83 maturation of PV neurons.

84 ***Results***

85 ***TRα1^{E395fs401X} expression in GABAergic neurons from an early developmental stage permanently***
86 ***inhibits PV neuron maturation***

87 In our previous work, we used Cre/loxP recombination to restrict the expression of the dominant-
88 negative TRα1^{L400R} mutant receptor in the GABAergic lineage from embryonic day 12.5 (16). As most
89 of the mice had frequent epileptic seizures and died before postnatal day 21 (PND21), we could not
90 address a possible recovery of PV neuron maturation during adulthood. We thus used here a similar
91 model, based on the *Thra^{Slox}* allele, encoding TRα1^{E395fs401X}, a receptor with moderate dominant-
92 negative activity (18). The floxed *ROSA-tdTomato^{lox}* reporter transgene was also introduced to trace
93 the cells belonging to the GABAergic lineage. One third of *Thra$^{Slox/+}$ ROSA-tdTomato$^{lox/+}$ Gad2-Cre* mice
94 survived to adulthood. We therefore compared these mutant mice and *Thra$^{+/+}$ ROSA-tdTomato$^{lox/+}$*
95 *Gad2-Cre* littermates (controls), to histologically study whether TRα1 mutation only delays or
96 permanently inhibits PV neuron maturation.

97 At PND21, while the red fluorescence did not indicate any cell loss in the GABAergic lineage
98 (Supplementary Fig. 1), the density of parvalbumin-positive (PV+) cells was drastically lower in
99 mutants than in controls (Fig. 1a, b). PNNs were labeled using Wisteria Floribunda Agglutinin (WFA),
100 which binds N-acetyl-galactosamine-β1 residues of PNN glycoproteins. The density of WFA-positive
101 (WFA+) cells was also significantly lower in mutants (Fig. 1a, c). Interestingly, the two phenotypes
102 were accompanied by a clearly lower ratio of PV+ cells that were surrounded by PNNs in mutants,
103 compared to controls (Fig. 1a, d). At adult stage, the same analysis showed signs of some recovery of
104 PV neuron density in mutants (Fig. 1e, f), while the PNN defect persisted (Fig. 1e, g and h). Overall,

105 TRα1^{E395fs401X} appears to have a similar negative influence to TRα1^{L400R} and permanently impairs the
106 maturation of PV neurons.

107 ***Postnatal expression of TRα1^{L400R} in GABAergic neurons is sufficient to inhibit PV neuron***
108 ***maturation***

109 We have recently observed that the postnatal expression of TRα1^{L400R} in PV neurons has little effect
110 on their maturation (Ren et al., 2024). Although adult *Thra$^{AMI/+}$ ROSA-tdTomato$^{lox/+}$ Pvalb-Cre* mice
111 displayed minor histological, electrophysiological and behavioral defects, they did not spontaneously
112 present epileptic seizures or lethality (19). This suggests that TH signaling intensively stimulates the
113 maturation of PV neurons during a specific time window, and then becomes secondary to maintain
114 their function. To better evaluate the temporal restriction of TH signaling for PV neurons maturation,
115 we used *Thra$^{AMI/+}$ ROSA-tdTomato$^{lox/+}$ Gad2-CreER^{T2}* mice (mutants) and *Thra$^{+/+}$ ROSA-tdTomato$^{lox/+}$*
116 *Gad2-CreER^{T2}* or *Gad2-CreER^{T2}* negative mice (controls), where Cre/loxP recombination can be
117 induced at a chosen time by tamoxifen treatment.

118 A first batch of these mice were treated with tamoxifen at PND7 and histological analysis was
119 performed at PND14. This analysis revealed that expressing TRα1^{L400R} during the second postnatal
120 week was sufficient to compromise the onset of parvalbumin expression (Fig. 2a, b). But the
121 amplitude of the defect in PV expression in mutant mice was not as high as that in our previous work,
122 where TH signaling was blocked from embryonic day 12.5 to PND14 in *Thra$^{AMI/+}$ ROSA-tdTomato$^{lox/+}$*
123 *Gad2-Cre* mice (16). Besides, we did not observe any clear change in either the density of WFA+ cells
124 (Fig. 2a, c) or the ratio of PV+ cells that were surrounded by PNNs (Fig. 2a, d). This may be due to the
125 fact that the elaboration of PNNs mainly takes place after PND14, so that the density of WFA+ cells
126 was low, with high interindividual variability. By contrast, a tamoxifen treatment performed during
127 the fourth postnatal week (from PND21 to PND25), did not cause any significant change in either PV+
128 cell density or WFA+ cell density at adult stage (Fig. 2e-h). Therefore, THs exert their influence during
129 a postnatal time window, which includes the second postnatal week and precedes weaning, since
130 weaning usually occurs after the end of the third postnatal week in mice.

131 ***Consequences of TRα1^{L400R} expression on gene expression in neocortical GABAergic neurons two***
132 ***weeks after birth***

133 We set out to analyze the influence of TRα1^{L400R} expression on the nuclear transcriptome of
134 GABAergic neurons at PND14, a developmental stage which appears to be quite central in the
135 timeline of TH action in PV neurons. To do this, we used the *ROSA-GSL10gfp^{lox}* reporter transgene,

136 which labels cell nuclei, to extract nuclear RNA from neocortical GABAergic neurons, in which PV
137 neurons represent around 50% of the population (20). RNA-seq analysis was performed for *Thra*$^{AMI/+}$
138 *ROSA-GSL10gfp*$^{lox/+}$ *Gad2-Cre* mice and *Thra*$^{+/+}$ *ROSA-GSL10gfp*$^{lox/+}$ *Gad2-Cre* control littermates at
139 PND14. Differential analysis (Deseq2 adjusted p-value > 0.05; fold-change >2.0; basemean > 30)
140 identified 275 down-regulated genes and 265 up-regulated genes in mutant mice. This large gene set
141 contains TRα1 target genes whose transcription is normally up-regulated by liganded TRα1. Notably,
142 among these were genes (*Hr, Klf9, Dbp, Shh, Gabrd*) that are known to be TRα1 target genes in other
143 cell types (21). However, many of the observed changes in mRNA level probably represent indirect
144 consequences of the long-term influence of TRα1^{L400R} expression on the cell physiology.

145 To distinguish direct TRα1 target genes from other genes that are downstream in the cascade, we
146 carried out a series of additional studies. First, we looked for genes which are down-regulated by
147 hypothyroidism and up-regulated at PND14 after a short TH treatment. To do this, we used a
148 propylthiouracyl (PTU) treatment to induce hypothyroidism in gestating females and their offspring.
149 Half of the hypothyroid pups with a *Thra*$^{+/+}$ *ROSA-GSL10gfp*$^{lox/+}$ *Gad2-Cre* genotype then received THs
150 at PND13. The nuclear RNA transcriptome of GABAergic neurons in the neocortex from hypothyroid
151 pups, and from pups treated with THs for 24 hours, was analyzed as above. In this setting we
152 expected a selective recovery of mRNA level for TRα1 target genes.

153 A total of 1306 genes were sensitive to either TRα1^{L400R} expression, hypothyroidism, or TH
154 stimulation (Fig. 3a, b). Among them, a large set of genes were only deregulated in hypothyroid mice.
155 This suggests an important influence of hypothyroidism on the microenvironment (notably glial cells)
156 of GABAergic neurons, with indirect consequences on gene expression in GABAergic neurons. The
157 genes whose expression in GABAergic neurons was sensitive to both TRα1^{L400R} expression and
158 hypothyroidism rather reflect the cell-autonomous influence of TH signaling in these neurons.
159 Importantly, among a total of 388 of such genes was the *Pvalb* gene, which encodes parvalbumin.
160 Recovery after TH treatment (TH response reached a two-fold threshold) was achieved for only a
161 small subset of these genes (61 genes up-regulated after TH treatment and 5 genes down-regulated
162 after TH treatment). However, clustering analysis revealed a clear trend toward recovery, which was
163 more visible for genes up-regulated by THs (Fig. 3c) than for genes down-regulated by THs (Fig. 3d).
164 The 5 genes which were down-regulated after TH treatment could reflect a poorly understood
165 negative regulation of transcription by the liganded TRα1 (Fig. 3b). In the end, only 61 genes behaved
166 as *bona fide* TRα1 target genes, with a robust negative response to both TRα1^{L400R} expression and
167 hypothyroidism, and a clear induction after the short TH treatment of hypothyroid mice (Fig. 3a).

168 Gene Ontology analysis indicated that many of the genes deregulated in hypothyroid and mutant
169 mice encode components of the extracellular matrix (GO:0031012; enrichment 4.4, p-value 3.10^{-13}).
170 This includes genes encoding collagens or proteins binding to the glycosaminoglycans of PNNs
171 (GO:0005539; enrichment 4.2, p-value 5.10^{-6}). This is consistent with the hypothesis that TH/TRα1
172 signaling stimulates the elaboration of PNNs around PV neurons. The expression of two of the
173 downregulated genes in this family (*Sema7a,* encoding semaphorin 7A and *Hapnl4,* encoding
174 hyaluronan and proteoglycan link protein 4) was restored after a short treatment with THs,
175 suggesting that they are TRα1 target genes.

176 Another prominent characteristic of deregulated genes in hypothyroid and mutant mice was the
177 presence of genes that encode voltage-gated potassium channels (GO:0005249; enrichment 6.1, p-
178 value 10^{-6}). As these genes appeared to be insensitive to acute TH treatment, their expression is
179 unlikely to be under the direct control of TRα1. This observation suggests that hypothyroidism or
180 long-term expression of $TR\alpha1^{L400R}$ in GABAergic neurons damage the postnatal remodeling of ions
181 channels, which is a key event for proper maturation of PV neurons in the neocortex (4). To further
182 evaluate this possibility, we extracted the genes that mostly encode ions channels and whose
183 expression is modified in this process of postnatal maturation as defined by Okaty and colleagues (4).
184 This analysis (Fig. 3e) revealed that this postnatal transition is impaired and that the immature status
185 of PV neurons persists in hypothyroid and mutant mice.

186 **Discussion**

187 In the present study, we extend our previous observations showing that a cell-autonomous action of
188 TH/TRα1 in GABAergic neurons is required for the maturation of neocortical PV neurons in mice. We
189 identified a time window that spans from birth to the end of the third postnatal week, during which
190 the action of THs is critical for the proper maturation of PV neurons. The analysis of gene expression
191 also pinpoints a set of genes that are directly regulated by TH/TRα1 in GABAergic neurons. Some of
192 these genes encode ion channels and PNN components, reflecting the involvement of THs in
193 essential steps of PV neuron maturation.

194 Using genetically modified mouse models expressing $TR\alpha1^{L400R}$, which exerts dominant negative
195 activity over TRα1, we have gathered evidence suggesting that the time window during which THs
196 promote PV neuron maturation is in the early postnatal weeks, notably during the second postnatal
197 week. First, blocking TH/TRα1 signaling in GABAergic neurons after PND7 is sufficient to alter the
198 expression of parvalbumin, as evidenced at PND14. On the contrary, blocking TH/TRα1 signaling in
199 GABAergic neurons after PND21 does not significantly alter PV neuron maturation, as assessed in

200 adulthood. PV neurons also show near-normal maturation when the blockade of TH/TRα1 signaling is
201 restricted to PV neurons and begins only after the onset of the expression of *Pvalb*, the gene that
202 encodes parvalbumin (19). Furthermore, a previous whole cortex RNA-seq analysis showed that gene
203 expression changes rapidly in wild-type mice during the second postnatal week and that this
204 evolution is stopped when TH/TRα1 signaling is blocked in GABAergic neurons (16). Finally, our novel
205 transcriptome analysis, which was carried out with sorted GABAergic neuron nuclei, indicates that
206 the postnatal maturation process of PV neurons is blunted by TRα1^{L400R} expression. In particular,
207 blocking TH/TRα1 signaling appears to compromise the expression of a number of genes involved in
208 a well-documented transition, during which the repertoire of ion channels is extensively modified
209 (Okaty et al., 2009). It is remarkable that the second postnatal week, during which THs seem to play a
210 crucial role in PV neuron maturation, coincides with a peak in circulating levels of THs (22). This
211 strongly suggests that THs represent a temporal cue to synchronize the postnatal maturation of PV
212 neurons.

213 The striking influence exerted by THs on cortical PV neuron maturation in the first postnatal weeks
214 does not exclude the possibility that THs also play a role in these neurons earlier during
215 development, or after weaning. First, we cannot fully rule out that TRα1 has an earlier function in PV
216 neurons, as recent observations suggest that it could act prenatally to promote the tangential
217 migration of GABAergic neuron progenitors (23). However, there is no indication that this effect is
218 exerted in a cell-autonomous manner. Second, the hypothesis that THs act mainly during the second
219 postnatal week is at odds with observations that were previously reported in mice expressing
220 TRα1^{R384C} in all tissues, for which a complete recovery in PV neuron density was observed in adults
221 (13). By contrast, in the present study we have observed little recovery in PV neuron maturation in
222 adult mice expressing TRα1^{E395fs401} in GABAergic neurons. This discrepancy is probably explained by
223 the residual capacity of TRα1^{R384C} to bind T3 and activate transcription (24), which is not the case for
224 TRα1^{E395fs401} (16). Therefore, the late onset of TRβ1 expression in PV neurons (25) does not appear to
225 be sufficient to counteract the influence of the dominant negative TRα1 mutated receptor.

226 The mode of TH action in PV neurons during the second postnatal week is clarified by RNA-seq data.
227 In the present study, we first found that PV neurons were much more sensitive to variations in TH
228 signaling at PND14 than at the adult stage, where the same method only showed minor changes in
229 gene expression (19). Another finding of the present study was that one prominent outcome of the
230 late maturation process of PV neurons, the elaboration of PNNs, appears to strongly rely on TH
231 signaling. Indeed, genes that were consistently deregulated when TH/TRα1 signaling was blocked,
232 encode extracellular matrix proteins, specific components of PNNs, or proteins interacting with PNN

233 glycosaminoglycans. We used rapid recovery of gene expression after TH treatment in hypothyroid
234 mice, as an indication of direct transcriptional control of gene expression by TRα1. This allowed us to
235 identify a small subset of genes whose deregulation is more likely to be the initial set of events
236 preventing PV neuron maturation. Among these are genes encoding transcription factors or cofactors
237 (*Dbp, Hr, Klf9*), that were already reported to be regulated by TRα1 in other contexts (21) and that
238 could act as upstream regulators of other deregulated genes. However, the presence in this subset of
239 putative TRα1 target genes of genes encoding components of PNNs suggests a more direct link
240 between TH and PNN content. Thus, it appears that liganded TRα1 might notably activate the
241 transcription of genes encoding collagens (*Col24a1* and *Col9a2* genes), ephrin A4 (*Epha4*), laminin
242 alpha 3 subunit (*Lama3*), semaphorin 7A (*Sema7a*) and hyaluronan and proteoglycan link protein 4
243 (*Hapln4* gene). This last protein notably represents an essential component of PNNs (26-28).

244 The novel data presented in this paper provide strong support for the hypothesis that TH is a major
245 temporal signal for the opening and closing of the critical period of heightened plasticity, as
246 previously suggested (29). The critical period occurs at slightly different times in different neocortical
247 areas, as does the onset of TH signaling (30). It is characterized by a series of cellular events that play
248 a crucial role in the elaboration of functional neuronal circuits (5). The beginning of parvalbumin
249 synthesis marks the opening of the critical period, while the elaboration of PNNs around PV neurons
250 stabilizes synapses and marks its closure. Thus, our findings suggest that both the opening and the
251 closure of the critical period are directly stimulated by liganded TRα1. Therefore, THs appear to act in
252 the postnatal neocortex as it does during amphibian metamorphosis, as an external cue that
253 represents an important temporal signal. During brain development, the influence of THs is also
254 found in glial cells, as TH signaling is particularly required for timely differentiation of
255 oligodendrocytes and myelin formation (12, 31). Of note, oligodendrocyte maturation has also been
256 shown to play a role in PV neuron maturation and in the closure of the critical period (32).

257 Patients with early TH deficiency caused by congenital hypothyroidism (33) or carrying TRα1
258 mutations (11) are currently treated with TH replacement therapy. Treatment can have a positive
259 influence on cognitive development only if it is initiated soon after birth. This is an indication that the
260 TH action on the maturation of the human neocortex is also restricted to an early temporal window.
261 An alteration in the timing in the critical period is also suspected to cause autism spectrum disorders
262 (8). In that regard, it is noticeable that some of the rare patients in whom *THRA* mutations have been
263 discovered were first diagnosed for autism spectrum disorders (34, 35). Within the framework of our
264 hypothesis, irreversible cognitive and neurological disorders that are associated with TH related

265 diseases are related to ASD symptoms and might also be regarded as consequences of a disruption of
266 the critical period of heightened plasticity.

267 *Study limitations*

268 The complete characterization of TRα1 target genes in PV neurons would require the definition of
269 chromatin occupancy by the receptor, as it informs of its presence on regulatory sequences. This is
270 not currently feasible with the small number of cells that are collected when sorting PV neurons from
271 mouse neocortex. Also, the histological methods that we have used only indirectly inform of the
272 timing of the critical period of heightened plasticity, which can be defined in a number of different
273 ways (36, 37).

274 **Methods**

275 *Mouse models and treatments*

276 Experiments involving the use of live animals for the current project were approved by local ethics
277 committees (C2EA015 and C2EA017) and subsequently authorized by the French Ministry of
278 Research (Projects #33279-2021082516194165 and #25496-2020032811174506). Mice were bred
279 and maintained at Plateau de Biologie Expérimentale de la Souris (SFR BioSciences Gerland - Lyon
280 Sud, France).

281 The *Thra*^{AMI} allele allows the expression of the dominant-negative TRα1^{L400R} after the Cre/loxP-
282 mediated deletion of a cassette with polyadenylation signals (38). *Thra*^{Slox} is identical, except for the
283 presence of a C-terminus frameshift mutation which leads to the expression of the dominant-
284 negative TRα1^{E395fs401X}. The *ROSA-tdTomato*^{lox} reporter transgene (also known as Ai9, MGI Cat#
285 4436851, RRID: MGI: 4436851) drives the Cre-dependent expression of a red fluorescent protein,
286 mainly localized in cytoplasm (39). The *ROSA-GSL10gfp*^{lox} transgene encodes the GS-EGFP-L10a
287 protein, which is a green fluorescent protein fused to the N-terminus part of the large subunit
288 ribosomal protein L10a, mainly localized in cell nuclei (19). All transgenes were in C57Bl6/J genetic
289 background. *Gad2-Cre* and *Gad2-CreER*^{T2} are knock-in alleles in which the Cre recombinase reading
290 frame is inserted into the *Gad2* gene in order to restrict the expression of the recombinase in
291 GABAergic neurons (40) . Recombination was induced in mice carrying the *Gad2-CreER*^{T2} transgene
292 by intraperitoneal injection of tamoxifen (T5648, Sigma, dissolved in sterile sunflower oil (10 mg/ml).
293 PND7 mice received a single 50 µL subcutaneous injection whereas 3-week-old mice received 5 daily
294 intraperitoneal injections (daily dose: 7.5 µL/g).

295 Gestating mice were fed for 2 weeks with iodine deficient food supplemented with 0.15% propyl-thio
296 uracyl (Envigo ref TD.95125) to cause deep hypothyroidism. TH levels were restored by a single
297 intraperitoneal injection in half of the pups (10 µg T4 + 1 µg T3 dissolved in 50 µL of phosphate buffer
298 saline, all chemicals from Sigma Aldrich France). The other PTU treated animals were injected with 50
299 uL of phosphate buffer saline.

300 *RNA-seq analysis from sorted nuclei*

301 Nuclei were isolated from individual cortex frozen in liquid nitrogen and nuclear RNA was extracted
302 as previously described (19). Nuclear RNA was extracted from sorted nuclei (RNeasy Micro Kit,
303 Qiagen ref 74004) and quantified using Tapestation4150 (Agilent). 1 ng RNA was reverse-transcribed
304 using the SMART-Seq v4 Low Input RNA kit (Takara). cDNA was quantified and qualified using Qubit
305 (Invitrogen) and Tapestation4150 (Agilent). Libraries were then prepared from 1 ng cDNA using the
306 Nextera XT DNA Library Kit (Illumina). Libraries were sequenced (> 2.10^7 reads/library) on a
307 Nextseq500 DNA sequencer (Illumina). Reads were aligned on the mouse genome (mm10 GRCm38
308 release) with Bowtie2 (Galaxy Version 2.4.2 + galaxy 0) (41). Count table was prepared using htseq-
309 count (Galaxy Version 0.9.1 + galaxy 1, mode union, feature type: gene) (42). Differential gene
310 expression analysis was performed with DEseq2 (Galaxy Version 2.1.8.3) (43) using the following
311 thresholds: False Discovery Rate < 0.05; p-adjusted value < 0.05; maximum adjusted basecount > 30;
312 fold-change > 2.0. Hierarchical clustering was performed using Euclidian distance and complete
313 distance with Clustvis (44). Gene Ontology analysis was performed with Gorilla (https://cbl-
314 gorilla.cs.technion.ac.il/).

315 *Brain slice collection*

316 Each mouse was given a lethal intraperitoneal injection (6 mL/kg) of a mixture of ketamine (33
317 mg/mL) and xylazine (6.7 mg/mL). The thorax was opened and each mouse was perfused with 3.7%
318 paraformaldehyde in 0.1 M phosphate buffer at room temperature. Each brain was dissected out,
319 immersed in fixative at 4°C for 3 h and then in phosphate buffered saline (PBS) at 4°C until sectioning.
320 Coronal sections (50 µm) were cut with the aid of a vibrating microtome (Integraslice 7550 SPDS,
321 Campden Instruments, Loughborough, UK), in PBS at room temperature. Brain sections were stored
322 at -20°C in cryoprotectant (30% ethylene glycol and 20% glycerol in 10 mM low-salt PBS).

323 *Brain slice histology*

324 Immunohistochemistry was performed on free-floating brain sections. For PV labeling, a mouse anti-
325 PV primary antibody (PARV19, Sigma P3088, 1:2000), and a secondary antibody made in donkey
326 (anti-mouse DyLight 633, ThermoFisher Scientific, 1:1000) were used. For the concurrent PNN
327 labeling, a biotinylated Wisteria floribunda lectin (WFL/WFA, Vector Laboratories B-1355, 20 µg/mL),
328 and Streptavidin coupled to DyLight 488 (Vector Laboratories, SA-5488, 1:1000) were used. Non-
329 specific binding sites were blocked by incubating sections for 1 h in PBS with 1% BSA and 0.2% Triton
330 X-100. Brain sections were incubated overnight at 4°C with PV antibody and biotinylated WFA, which
331 were diluted in PBS with 1% BSA, 0.2% Triton X-100 and 1% dimethyl sulfoxide. Sections were
332 washed in PBS and further incubated for 15 min at room temperature with DAPI (4',6-diamidino-2-
333 phenylindole, 1:5000, Sigma). Incubation with the secondary antibody lasted for 3 h at room
334 temperature. Sections were mounted in Fluoroshield™ (Sigma), coverslipped and imaged using an
335 inverted confocal microscope (Zeiss LSM 780 and Zeiss LSM 800).

336 *Image analysis*

337 Image analysis was performed using ImageJ. Final images resulted from the z projection of 3 optical
338 sections (Maximum intensity tool) that were 2 µm apart (the resulting images thus reflected the
339 fluorescence collected over a thickness of 4 µm). The densities of Tomato+, PV+, WFA+ cells, and
340 their co-localizations were measured in the whole area of one image taken in the somatosensory
341 cortex area. Three to four images in both hemispheres were analyzed for each mouse. Except for Fig.
342 2a-d, for which the counting was performed manually, the Cellpose wrapper for Fiji (45) was used to
343 count Tomato+, PV+ and WFA+ cells. Numbers of mono-, double- or triple-labelled cells per slice
344 were measured automatically. The code of the original macro may be found here:
345 https://github.com/jbrocardplatim/MacroPV.

346 Quantitative data were analyzed using two-tailed unpaired T-test. Data are expressed as mean ±
347 SEM. Data analyses were performed with Excel 2016 and GraphPad Prism software (v.8.). The level of
348 significance was set at $p < 0.05$.

349 **Figure legends:**

350 **Fig. 1 | Persistent defect in PV neuron maturation in mice expressing TRα1^{E395fs401X}.** Histological
351 analysis of *Thra*$^{+/+}$ *ROSA-tdTomato*$^{lox/+}$ *Gad2-Cre* littermates (controls) and *Thra*$^{Slox/+}$ *ROSA-*
352 *tdTomato*$^{lox/+}$ *Gad2-Cre* mice (mutants) that express TRα1^{E395fs401X} in the GABAergic neurons and their
353 progenitors from embryonic day 12.5 to PND21 (**a-d**, controls: n = 6, mutants: n = 6) and to adult
354 stage (**e-h**, controls: n = 6, mutants: n = 5). **a, e** Immunohistochemistry of parvalbumin and WFA-

355 labeled PNNs in PV neurons of somatosensory cortex at striatum level. **b, f** The density of PV+ cells
356 was lower in mutants at both ages. **c, g** The density of WFA+ cells was lower in mutants at both ages.
357 **d, h** The proportion of PV neurons surrounded by PNNs was lower in mutants at both ages. Data are
358 presented as mean ± SEM and analyzed using an unpaired two-tailed T-test (*$p < 0.05$, **$p < 0.01$,
359 ***$p < 0.001$).

360 **Fig. 2 | A time window for TH action on PV neuron maturation.** Histological analysis of *Thra*$^{+/+}$ *ROSA-*
361 *tdTomato*$^{lox/+}$ *Gad2-CreER*^{T2} or *Gad2-CreER*^{T2} negative littermates (controls) and *Thra*$^{AMI/+}$ *ROSA-*
362 *tdTomato*$^{lox/+}$ *Gad2-CreER*^{T2} mice (mutants) that express TRα1^{L400R} in the GABAergic neurons from
363 PND7 to PND14 (**a-d**, controls: n = 8, mutants: n = 6) and from PND21 to adult (**e-h**, controls: n = 11,
364 mutants: n = 7). **a, e** Immunohistochemistry of parvalbumin and WFA-labeled PNNs in PV neurons of
365 somatosensory cortex at striatum level. **b, f** The density of PV+ cells was lower in mutants in former
366 but not in latter. **c, g** The density of WFA+ cells had no clear difference in both cases. **d, h** The
367 proportion of PV neurons surrounded by PNNs had no clear difference in both cases. Data are
368 presented as mean ± SEM and analyzed using unpaired two-tailed T-test (*$p < 0.05$, **$p < 0.01$, ***p
369 < 0.001).

370 **Fig. 3 | RNA-seq analysis of gene expression in sorted GABAergic neuron nuclei.** Nuclei were sorted
371 at PND14 from the neocortex of *Thra*$^{+/+}$ *ROSA-GSL10gfp*^{lox} *Gad2-Cre* mice (Ctrl), *Thra*$^{AMI/+}$ *ROSA-*
372 *GSL10gfp*^{lox} *Gad2-Cre* mice expressing TRα1^{L400R} in GABAergic neurons (Mut), hypothyroid *Thra*$^{+/+}$
373 *ROSA-GSL10gfp*^{lox} *Gad2-Cre* mice (Hypoth.), or hypothyroid *Thra*$^{+/+}$ *ROSA-GSL10gfp*^{lox} *Gad2-Cre* mice
374 that received a single TH injection at PND13 (+TH). **a** Venn diagram of genes that were either
375 downregulated by TRα1^{L400R}, downregulated by hypothyroidism or upregulated after TH treatment. **b**
376 Venn diagram of genes that were either upregulated by TRα1^{L400R}, upregulated by hypothyroidism or
377 downregulated after TH treatment (thresholds: Fold change > 2 or < 0.5, maximal adjusted base
378 counts > 30, adjusted p-value > 0.05). **c** Heatmap showing the genes that were downregulated by
379 both TRα1^{L400R} and hypothyroidism. Note the variable response to TH. **d** Heatmap showing the genes
380 that were upregulated by both TRα1^{L400R} and hypothyroidism. **e** Heatmap of markers of PV neuron
381 maturation. The marks on the right side are for genes whose expression normally increases (red) or
382 decreases (green) between PND7 and PND21. The alterations of gene expression in mutant mice
383 reveals a blockade of the PV neuron maturation program, caused either by TRα1^{L400R} expression or by
384 hypothyroidism. A 24h TH treatment two weeks after birth is not sufficient to restore the expression
385 of these marker genes.

386

387

Acknowledgements:

We acknowledge the contribution of SFR Biosciences (Université Claude Bernard Lyon 1, CNRS UAR3444, Inserm US8, ENS de Lyon): Nadine Aguilera and the Plateau de Biologie Expérimentale de la Souris (ANIRA-PBES) for mouse breeding; Sébastien Dussurgey from ANIRA-Cytométrie for nuclei sorting; ANIRA-AGC for mouse genotyping; LyMIC-PLATIM for imaging. We thank Benjamin Gillet and Sandrine Hughes of the deep sequencing facility (PSI IGFL, Lyon). We also thank Elodie Martel for carrying out histology experiments as part of her internships and Isabelle Dusart (Institut de Biologie Paris Seine, France) for helpful discussions. We acknowledge China Scholarship Council for a scholarship to Juan REN to do her PhD project in ENS de Lyon. Research fundings were from European Union's Horizon 2020 research and innovation program, under grant agreement No. 825753 (ERGO), Agence Nationale de la Recherche (Thyromut2 program; ANR-15-CE14-0011-01).

Declaration of interest

No conflict of interest

References

1. S. Hijazi, A. B. Smit, R. E. van Kesteren, Fast-spiking parvalbumin-positive interneurons in brain physiology and Alzheimer's disease. *Mol Psychiatry* **28**, 4954-4967 (2023).
2. J. A. del Rio, L. de Lecea, I. Ferrer, E. Soriano, The development of parvalbumin-immunoreactivity in the neocortex of the mouse. *Brain Res Dev Brain Res* **81**, 247-259 (1994).
3. Z. J. Huang *et al.*, BDNF regulates the maturation of inhibition and the critical period of plasticity in mouse visual cortex. *Cell* **98**, 739-755 (1999).
4. B. W. Okaty, M. N. Miller, K. Sugino, C. M. Hempel, S. B. Nelson, Transcriptional and electrophysiological maturation of neocortical fast-spiking GABAergic interneurons. *J Neurosci* **29**, 7040-7052 (2009).
5. T. K. Hensch, Critical period plasticity in local cortical circuits. *Nat Rev Neurosci* **6**, 877-888 (2005).
6. A. E. Takesian, T. K. Hensch, Balancing plasticity/stability across brain development. *Prog Brain Res* **207**, 3-34 (2013).
7. J. C. Wingert, B. A. Sorg, Impact of Perineuronal Nets on Electrophysiology of Parvalbumin Interneurons, Principal Neurons, and Brain Oscillations: A Review. *Frontiers in synaptic neuroscience* **13**, 673210 (2021).
8. V. S. Sohal, J. L. R. Rubenstein, Excitation-inhibition balance as a framework for investigating mechanisms in neuropsychiatric disorders. *Mol Psychiatry* **24**, 1248-1257 (2019).
9. F. Flamant, K. Gauthier, Thyroid hormone receptors: the challenge of elucidating isotype-specific functions and cell-specific response. *Biochim Biophys Acta* **1830**, 3900-3907 (2013).
10. P. Berbel, D. Navarro, G. C. Roman, An evo-devo approach to thyroid hormones in cerebral and cerebellar cortical development: etiological implications for autism. *Frontiers in endocrinology* **5**, 146 (2014).

11. A. L. M. van Gucht *et al.*, Resistance to Thyroid Hormone due to Heterozygous Mutations in Thyroid Hormone Receptor Alpha. *Current topics in developmental biology* **125**, 337-355 (2017).
12. F. Picou, T. Fauquier, F. Chatonnet, S. Richard, F. Flamant, Deciphering direct and indirect influence of thyroid hormone with mouse genetics. *Mol Endocrinol* **28**, 429-441 (2014).
13. K. Wallis *et al.*, Locomotor deficiencies and aberrant development of subtype-specific GABAergic interneurons caused by an unliganded thyroid hormone receptor alpha1. *J Neurosci* **28**, 1904-1915 (2008).
14. K. Uchida *et al.*, Thyroid hormone insufficiency alters the expression of psychiatric disorder-related molecules in the hypothyroid mouse brain during the early postnatal period. *Scientific reports* **11**, 6723 (2021).
15. S. Mayerl, H. Heuer, Thyroid hormone transporter Mct8/Oatp1c1 deficiency compromises proper oligodendrocyte maturation in the mouse CNS. *Neurobiol Dis* **184**, 106195 (2023).
16. S. Richard *et al.*, A Pivotal Genetic Program Controlled by Thyroid Hormone during the Maturation of GABAergic Neurons. *iScience* **23**, 100899 (2020).
17. M. E. Gilbert *et al.*, Thyroid hormone insufficiency during brain development reduces parvalbumin immunoreactivity and inhibitory function in the hippocampus. *Endocrinology* **148**, 92-102 (2007).
18. S. Markossian *et al.*, CRISPR/Cas9 Editing of the Mouse Thra Gene Produces Models with Variable Resistance to Thyroid Hormone. *Thyroid* **28**, 139-150 (2018).
19. J. Ren *et al.*, Thyroid hormones maintain parvalbumin neuron functions in mouse neocortex. *bioRxiv* 10.1101/2024.07.16.603713, 2024.2007.2016.603713 (2024).
20. B. Tasic *et al.*, Adult mouse cortical cell taxonomy revealed by single cell transcriptomics. *Nat Neurosci* **19**, 335-346 (2016).
21. Y. Zekri, R. Guyot, F. Flamant, An Atlas of Thyroid Hormone Receptors' Target Genes in Mouse Tissues. *International journal of molecular sciences* **23** (2022).
22. S. Friedrichsen *et al.*, Regulation of iodothyronine deiodinases in the Pax8-/- mouse model of congenital hypothyroidism. *Endocrinology* **144**, 777-784 (2003).
23. E. da Cunha Menezes *et al.*, Effects of gestational hypothyroidism on mouse brain development: Gabaergic systems and oxidative stress. *Dev Biol* **515**, 112-120 (2024).
24. A. Tinnikov *et al.*, Retardation of post-natal development caused by a negatively acting thyroid hormone receptor alpha1. *Embo J* **21**, 5079-5087 (2002).
25. D. R. Hochbaum *et al.*, Thyroid hormone remodels cortex to coordinate body-wide metabolism and exploration. *Cell* **187**, 5679-5697 e5623 (2024).
26. K. Nojima, H. Miyazaki, T. Hori, L. Vargova, T. Oohashi, Assessment of Possible Contributions of Hyaluronan and Proteoglycan Binding Link Protein 4 to Differential Perineuronal Net Formation at the Calyx of Held. *Front Cell Dev Biol* **9**, 730550 (2021).
27. M. Edamatsu *et al.*, Hapln4/Bral2 is a selective regulator for formation and transmission of GABAergic synapses between Purkinje and deep cerebellar nuclei neurons. *J Neurochem* **147**, 748-763 (2018).
28. J. Popelar *et al.*, The absence of brain-specific link protein Bral2 in perineuronal nets hampers auditory temporal resolution and neural adaptation in mice. *Physiological research / Academia Scientiarum Bohemoslovaca* **66**, 867-880 (2017).
29. G. Batista, T. K. Hensch, Critical Period Regulation by Thyroid Hormones: Potential Mechanisms and Sex-Specific Aspects. *Front Mol Neurosci* **12**, 77 (2019).
30. L. Quignodon *et al.*, Thyroid hormone signaling is highly heterogeneous during pre- and postnatal brain development. *J Mol Endocrinol* **33**, 467-476 (2004).
31. B. Durand, M. Raff, A cell-intrinsic timer that operates during oligodendrocyte development. *Bioessays* **22**, 64-71 (2000).
32. B. T. Kalish *et al.*, Single-nucleus RNA sequencing of mouse auditory cortex reveals critical period triggers and brakes. *Proc Natl Acad Sci U S A* **117**, 11744-11752 (2020).

33. G. Van Vliet, J. Deladoey, Diagnosis, treatment and outcome of congenital hypothyroidism. *Endocr Dev* **26**, 50-59 (2014).
34. R. K. Yuen *et al.*, Whole-genome sequencing of quartet families with autism spectrum disorder. *Nat Med* **21**, 185-191 (2015).
35. M. K. Kalikiri, M. P. Mamidala, A. N. Rao, V. Rajesh, Analysis and functional characterization of sequence variations in ligand binding domain of thyroid hormone receptors in autism spectrum disorder (ASD) patients. *Autism research : official journal of the International Society for Autism Research* 10.1002/aur.1838 (2017).
36. K. B. Quast *et al.*, Rapid synaptic and gamma rhythm signature of mouse critical period plasticity. *Proc Natl Acad Sci U S A* **120**, e2123182120 (2023).
37. R. K. Reh *et al.*, Critical period regulation across multiple timescales. *Proc Natl Acad Sci U S A* **117**, 23242-23251 (2020).
38. L. Quignodon, S. Vincent, H. Winter, J. Samarut, F. Flamant, A point mutation in the activation function 2 domain of thyroid hormone receptor alpha1 expressed after CRE-mediated recombination partially recapitulates hypothyroidism. *Mol Endocrinol* **21**, 2350-2360 (2007).
39. L. Madisen *et al.*, A robust and high-throughput Cre reporting and characterization system for the whole mouse brain. *Nat Neurosci* **13**, 133-140 (2010).
40. H. Taniguchi *et al.*, A resource of Cre driver lines for genetic targeting of GABAergic neurons in cerebral cortex. *Neuron* **71**, 995-1013 (2011).
41. B. Langmead, C. Trapnell, M. Pop, S. L. Salzberg, Ultrafast and memory-efficient alignment of short DNA sequences to the human genome. *Genome Biol* **10**, R25 (2009).
42. S. Anders, P. T. Pyl, W. Huber, HTSeq--a Python framework to work with high-throughput sequencing data. *Bioinformatics* **31**, 166-169 (2015).
43. M. I. Love, W. Huber, S. Anders, Moderated estimation of fold change and dispersion for RNA-seq data with DESeq2. *Genome Biol* **15**, 550 (2014).
44. T. Metsalu, J. Vilo, ClustVis: a web tool for visualizing clustering of multivariate data using Principal Component Analysis and heatmap. *Nucleic Acids Res* **43**, W566-570 (2015).
45. C. Stringer, T. Wang, M. Michaelos, M. Pachitariu, Cellpose: a generalist algorithm for cellular segmentation. *Nat Methods* **18**, 100-106 (2021).

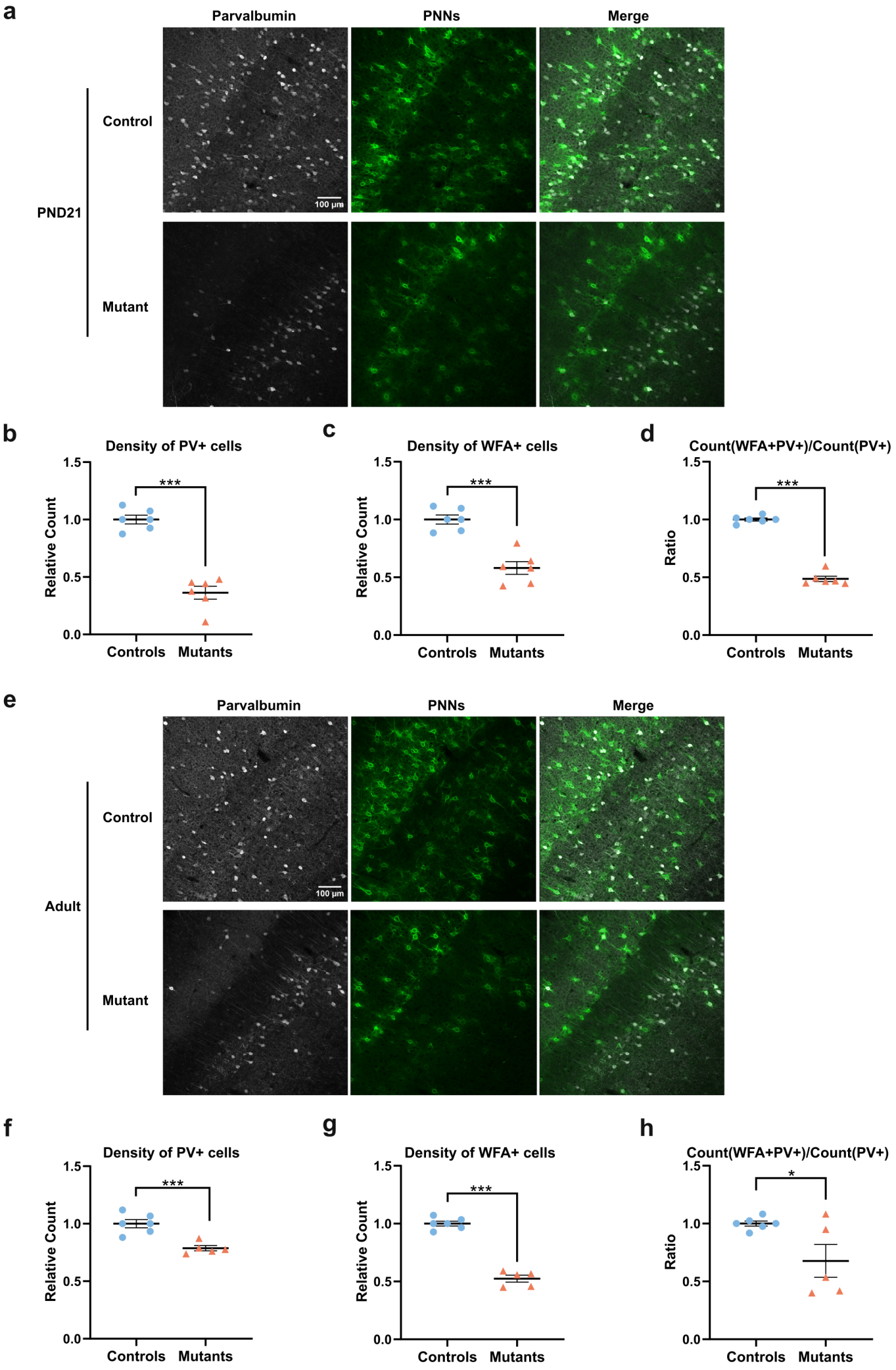
a
Parvalbumin
PNNs
Merge
PND21
Control
Mutant
100 µm
b
Density of PV+ cells
Relative Count
1.5
1.0
0.5
0.0
***
Controls
Mutants
c
Density of WFA+ cells
Relative Count
1.5
1.0
0.5
0.0
***
Controls
Mutants
d
Count(WFA+PV+)/Count(PV+)
Ratio
1.5
1.0
0.5
0.0
***
Controls
Mutants
e
Parvalbumin
PNNs
Merge
Adult
Control
Mutant
100 µm
f
Density of PV+ cells
Relative Count
1.5
1.0
0.5
0.0
***
Controls
Mutants
g
Density of WFA+ cells
Relative Count
1.5
1.0
0.5
0.0
***
Controls
Mutants
h
Count(WFA+PV+)/Count(PV+)
Ratio
1.5
1.0
0.5
0.0
*
Controls
Mutants

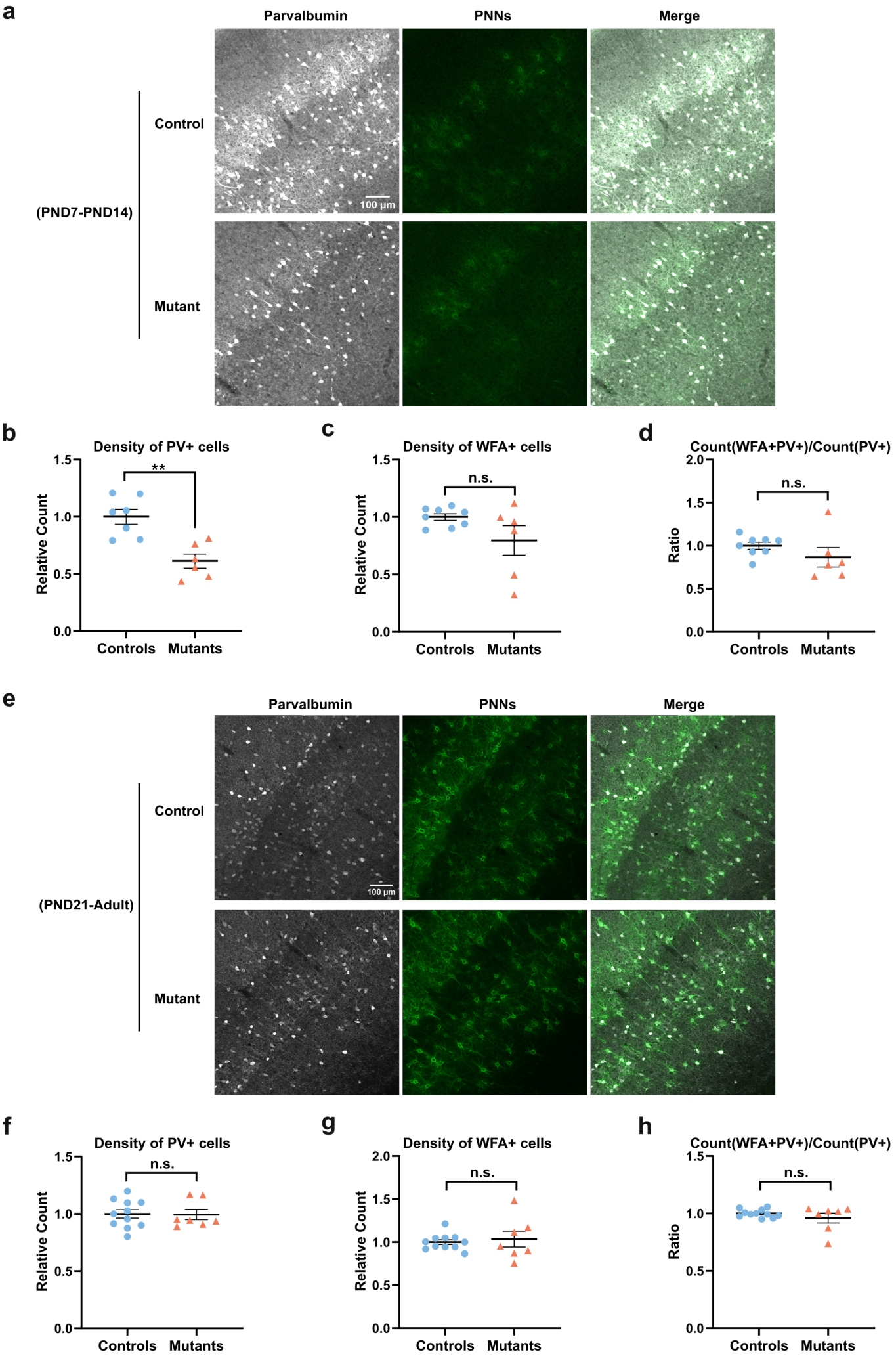
a
Parvalbumin
PNNs
Merge
Control
(PND7-PND14)
Mutant
100 µm
b
Density of PV+ cells
Relative Count
**
Controls
Mutants
c
Density of WFA+ cells
Relative Count
n.s.
Controls
Mutants
d
Count(WFA+PV+)/Count(PV+)
Ratio
n.s.
Controls
Mutants
e
Parvalbumin
PNNs
Merge
Control
(PND21-Adult)
Mutant
100 µm
f
Density of PV+ cells
Relative Count
n.s.
Controls
Mutants
g
Density of WFA+ cells
Relative Count
n.s.
Controls
Mutants
h
Count(WFA+PV+)/Count(PV+)
Ratio
n.s.
Controls
Mutants

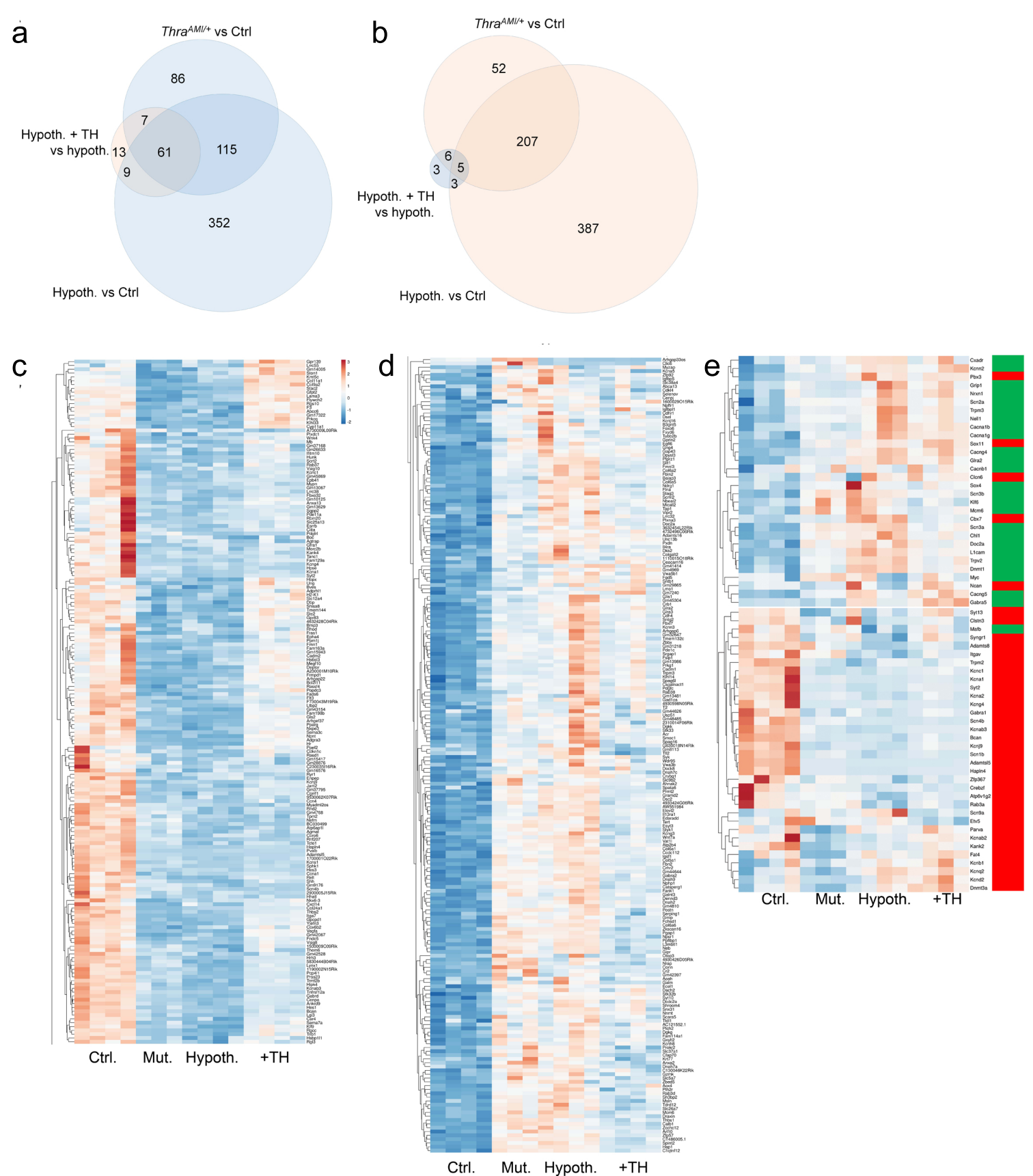
a
Thra^AMI/+ vs Ctrl
86
7
Hypoth. + TH
vs hypoth.
13
61
115
9
352
Hypoth. vs Ctrl
b
Thra^AMI/+ vs Ctrl
52
207
6
3
5
3
Hypoth. + TH
vs hypoth.
387
Hypoth. vs Ctrl
c
Ctrl.
Mut.
Hypoth.
+TH
d
Ctrl.
Mut.
Hypoth.
+TH
e
Ctrl.
Mut.
Hypoth.
+TH